Point defects controlling non-radiative recombination in GaN blue light emitting diodes: Insights from radiation damage experiments

In-Hwan Lee,[1] A. Y. Polyakov,[2] N. B. Smirnov,[2] I. V. Shchemerov,[2] P. B. Lagov,[2] R. A. Zinov'ev,[2] E. B. Yakimov,[2,3] K. D. Shcherbachev,[2] and S. J. Pearton[4,a)]
[1]*Department of Materials Science and Engineering, Korea University Anamro 145, Seoul 02841, South Korea*
[2]*National University of Science and Technology MISiS, Moscow, Leninskiy pr. 4, Moscow 119049, Russia*
[3]*Institute of Microelectronics Technology and High Purity Materials Russian Academy of Science, Chernogolovka, Moscow dist. 142432, Russia*
[4]*Department of Materials Science and Engineering, University of Florida, Gainesville, Florida 32611, USA*

(Received 20 August 2017; accepted 6 September 2017; published online 21 September 2017)

The role of Shockley-Read-Hall non-radiative recombination centers on electroluminescence (EL) efficiency in blue multi-quantum-well (MQW) 436 nm GaN/InGaN light emitting diodes (LEDs) was examined by controlled introduction of point defects through 6 MeV electron irradiation. The decrease in the EL efficiency in LEDs subjected to irradiation with fluences above 5×10^{15} cm^{-2} was closely correlated to the increase in concentration of E_c-0.7 eV electron traps in the active MQW region. This increase in trap density was accompanied by an increase in the both diode series resistance and ideality factor (from 1.4 before irradiation to 2.1 after irradiation), as well as the forward leakage current at low forward voltages that compromise the injection efficiency. Hole traps present in the blue LEDs do not have a significant effect on EL changes with radiation because of their low concentration. *Published by AIP Publishing*. [http://dx.doi.org/10.1063/1.5000956]

I. INTRODUCTION

Multi-quantum-well (MQW) III-Nitride light emitting diodes (LEDs) are widely used in the visible-UV spectral range and are efficient solid-state light sources for multiple applications.[1–5] The internal quantum efficiency (IQE) of these devices is determined by the ratio of the electron-hole pairs recombining via the band-to-band radiative recombination mode to the total number of recombining nonequilibrium charge carriers.[6] This efficiency is often analyzed in terms of the so-called ABC model[6,7] in which coefficients A, B, and C describe the contributions to recombination of charge carriers via the Shockley-Read-Hall (SRH) mechanism,[6] the band-to-band radiative recombination,[6] and the non-radiative Auger mechanism,[8] respectively. The non-radiative SRH recombination determines the peak IQE value of LEDs as a function of the drive current, while the decrease of IQE at high drive currents is often associated with the Auger recombination.[6]

There is still debate about the properties and nature of the SRH centers in III-Nitrides. The situation is best understood for GaN where it has been shown experimentally that non-radiative recombination on dislocations plays an important role for dislocation densities of $\sim 10^9$ cm^{-2} or higher[9,10] while for lower dislocation densities, the average diffusion lengths/lifetimes of charge carriers correlate with the concentration of E_c–0.56 eV electron traps[10,11] or in irradiated materials, with the density of major radiation defects with levels near E_c–1 eV.[12] The former are important in the decrease of radiative recombination efficiency of non-polar GaN films grown under non-optimal conditions.[13] These traps have also been shown to figure prominently in current collapse of electrically stressed GaN-based transistors.[14–16] The E_c–1 eV centers have been ascribed to deep acceptors due to interstitial nitrogen N_i^-.[17] Iron doping used for creating high-resistivity GaN films[17] creates deep traps near E_c–(0.5–0.6) eV attributed to the charge transfer level F^{3+}/Fe^{2+}.[18,19] These centers are effective non-radiative recombination centers.[19]

For GaN/InGaN MQW LED structures, experimental data are scarce. For the structures with emission wavelength from 390 nm (NUV) to 430 nm (blue) and 515 nm (green), the deep level spectra are dominated by electron and hole traps in the active MQW region.[20] The energy levels of the traps are approximately tied to the level of vacuum and associated with N_i^- acceptors in n-GaN and with multilevel gallium vacancy V_{Ga} acceptor complexes with shallow donors V_{Ga}-D.[17,21,22] Studies of NUV LEDs after electric degradation[23,24] or electron irradiation[25] showed that the changes in external quantum efficiency (EQE) are correlated to the increase in the density of the deep electron traps at Ec-(0.7–0.8) eV in the MQW region. For blue LEDs, changes in EQE of various LEDs can be associated with the changes in concentration of electron traps E_c–(0.5–0.6) eV and/or E_c–(0.6–0.7) eV in the MQW region, but relative contributions of these two types of traps could not be established.[26,27]

First principles calculations of non-radiative charge recombination in wide-bandgap materials was carried out for the multiphonon mechanism considering hole capture processes in n-GaN via multicharge carbon on nitrogen sites C_N^- acceptors.[28] This showed that the hole capture by such centers is very efficient, leading to hole capture coefficients on the order of 10^{-7}–10^{-6} cm^3/s (hole capture cross sections of 10^{-14}–10^{-13} cm^2). However, the electron capture by these centers was very slow because of the distance of the levels to the conduction band edge (the probability of capture in the multiphonon process decreases exponentially with the depth

a)Author to whom correspondence should be addressed: spear@mse.ufl.edu

of the level[28]). The role of multicharge V_{Ga}-D complexes with charge transfer levels -/0 near $E_v+1.2$ eV and 0/+ near E_v+1 eV on capture of holes and electrons showed that the lowermost charge states were effective in capturing holes in GaN, but the capture of electrons was slow because of the high distance from the level to the conduction band.[6] These predictions correspond with the hole and electron capture cross sections measured experimentally for the main hole traps in n-GaN by deep level transient spectroscopy (DLTS)[10,29] or time resolved photoluminescent (TRPL) spectroscopy.[30,31] The conclusion is that the hole traps cannot be efficient SRH centers in GaN, but as the InGaN bandgap becomes narrower with increasing In content, they might start playing a role in In-rich green LEDs.[6] Even for relatively shallow Fe-related E_c–0.5 eV centers, the capture coefficients for electrons and holes can be similarly high if processes involving excited states are taken into account.[32,33]

Thus, it is clear that, while assessing the role of SRH centers in LED performance is important, additional experimental and theoretical studies are needed. In this paper, we present results for blue MQW GaN/InGaN LEDs. Additional deep traps in a controlled fashion by electron irradiation, allowing us to trace the changes in the EL to the changes in deep level concentrations. This has been done previously for NUV LEDs.[24,25] Although the problem of increasing the IQE values for blue LEDs is not as acute as for NUV or green LEDs, a better understanding of the processes underlying SRH recombination in GaN-based LEDs is useful in improving LEDs in the whole spectral range covered by this materials system.

II. EXPERIMENTAL

The GaN/InGaN MQW LEDs were grown by metalorganic chemical vapor deposition (MOCVD) on basal plane patterned sapphire substrates (PSS). First 4-μm of undoped GaN was grown. The growth was then interrupted, the sample taken out from the reactor, dry etched via a Ni nanomask[27,34] down to 1 μm to form GaN nanopillars, and filled with SiO_2 nanoparticles (diameter 100 nm) by spin-coating. The GaN nanopillars had diameter of 100–150 nm and average density of $\sim 1.5\times10^9$ cm^{-2}. The growth was resumed to form 5–μm-thick n^+GaN doped with Si to 4×10^{18} cm^{-3}. The MQW active layer consisted of 5 undoped QWs of InGaN(2 nm)/GaN(10 nm), followed by Mg-doped 120-nm-thick p-GaN top contact layer. The structures were processed into 600×600 μm^2 chips by dry etching followed by mesa surface passivation. The p-type contact was made by indium tin oxide layer deposition followed by Ag top contact electrode deposition. The bottom n-type Ohmic contact employed standard lithographically patterned Al/Au annealed at 450 °C. The contact pattern was formed by standard photolithography. The chips were wire-bonded to sample holders.[27,34] Crystal quality was characterized by measuring the half-width of the symmetrical (0002) and asymmetrical (10–12) triple-axis high resolution x-ray diffraction (HRXRD) rocking curves to assess screw-component and edge dislocations, respectively.[35] These were performed using a D8 Discover (Bruker-AXS, Germany) diffractometer with Cu K_α radiation with $\lambda=1.5418$ Å. The dislocation density was also assessed by counting dark spot defects in room temperature microcathodoluminescence (MCL) images.[36,37] Further characterization involved capacitance-voltage (C-V), current-voltage (I-V), optical light output dependence on drive current (L-I), admittance spectroscopy (AS),[38] DLTS with electrical and optical (ODLTS) injection,[39] MCL spectra, electroluminescence (EL) spectra, and intensity as a function of the LED drive current. Electrical characteristics, DLTS/ODLTS spectra, and AS spectra measurements were performed in the 77–400 K temperature range using a gas-flow cryostat. For optical excitation in ODLTS, high-power commercial LEDs with wavelengths ranging from 940 nm to 365 nm were used.[10,12,29,40] LEDs were measured before and after irradiation with 6 MeV electrons produced by a linear accelerator. The irradiation was done at nominally room temperature, at an electron flux of 10^{11} cm^{-2}s^{-1} for which no sample heating by the incident electron beam was expected. The total electron fluences were 10^{15}, 2×10^{15}, 5×10^{15}, 1.5×10^{16}, 3×10^{16}, and 3.5×10^{16} cm^{-2}.

III. RESULTS

The epi structures had dislocation density $<10^8$ cm^{-2} and FWHM of the symmetrical (0002) and asymmetrical (10–12) HRXRD rocking curves of 271 arcseconds and 358 arcseconds, respectively. The low dislocation density results from the predominantly lateral overgrowth mode over the SiO_2 nanoparticles in the nanopillar GaN sublayer.[27,34] The peak of room temperature MQW-related MCL and EL spectra was 436 nm. Room temperature I-V characteristics [see Figs. 1(a) and 1(b)] showed an ideality factor of 1.4, with series resistance in the forward direction of 4.3Ω [Fig. 1(b)]. The reverse current at room temperature was $\sim10^{-11}$ A [Fig. 1(a)]. The internal quantum efficiency was determined as the ratio of the QW MCL intensity peak at 77 K to the room temperature intensity.[27,34] These measurements provide a lower boundary of the IQE[6] of 64%.

C-V profiling showed the edge of the space charge region (SCR) was below the lowermost InGaN QW at 0 V. To sweep the edge of the SCR through the lowest QW, the forward voltage was increased from 0.5 V to 2.5 V[27] (Fig. 2 shows the actual concentration profile). To probe the deep traps specifically within the MQW region, the DLTS and ODLTS spectra were recorded at quiescent bias of 0.5 V with forward pulsing to +2 V in the case of DLTS to ensure electron traps within the lowermost InGaN QW or at the InGaN/GaN interface of this well were probed. For hole traps within the QW, the photon energy of the excitation light in ODLTS was close to the QW bandgap (the actual wavelength LED used for excitation was 455 nm). The resultant spectra were then compared for the excitation with the LEDs creating electron-hole pairs both in the InGaN QWs and in GaN barriers. At temperatures below ~150 K, a strong capacitance freeze-out caused by the freeze-out of holes on Mg acceptors in the p-GaN contact layer gave rise to strong capacitance decrease with decreasing temperature at the DLTS frequency of 1 MHz.[10,12,27,29,40] This prevented accurate DLTS measurements in the low temperature region and necessitated use of a reduced frequency of 30–50 kHz.[27] In unirradiated samples, no electron traps

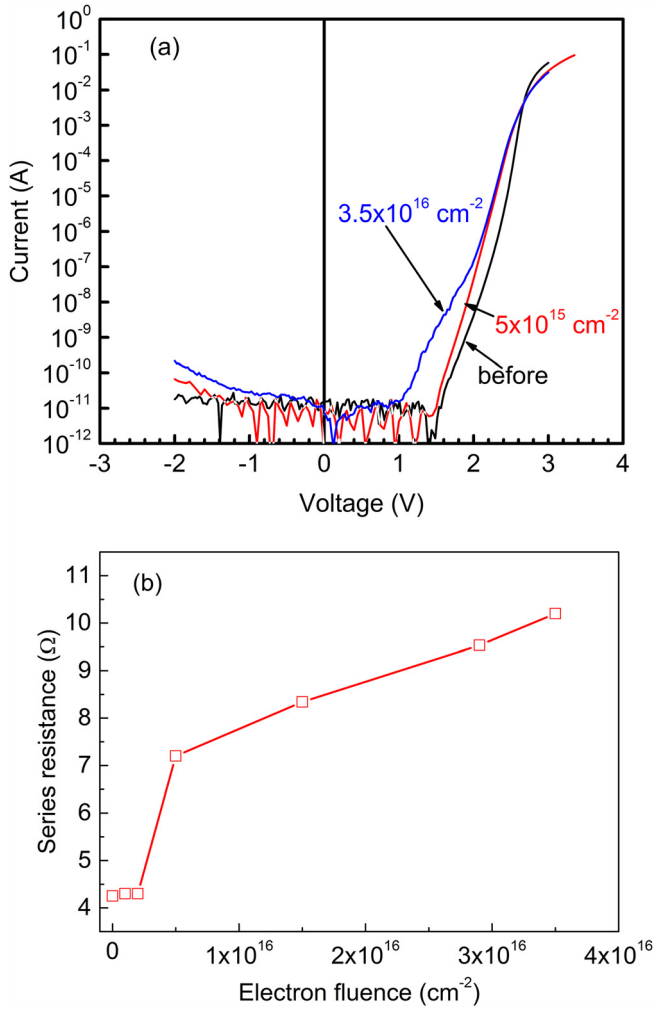

FIG. 1. (a) Room temperature I-V characteristics of the blue LEDs before electron irradiation (black line), after irradiation with fluence 5×10^{15} cm^{-2} (red line), and after irradiation with fluence of 3.5×10^{16} cm^{-2} (blue line); (b) dependence on electron fluence of the series resistance in forward direction.

could be reliably detected for the temperature range below 200 K even when DLTS spectra were taken at low probe frequency. Only for samples irradiated with high electron fluences could electron traps be detected at low temperatures.

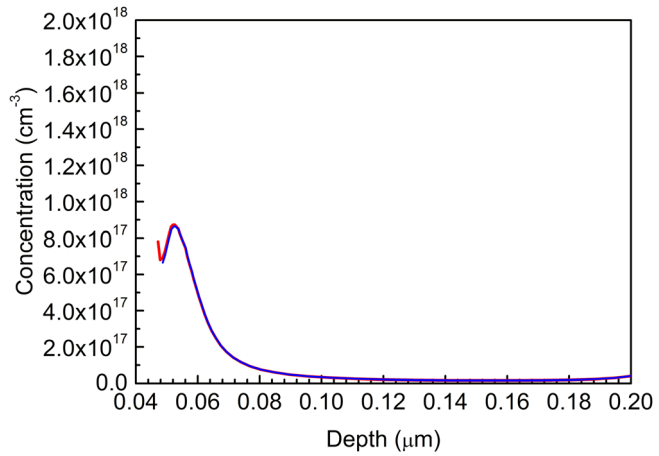

FIG. 2. Concentration profiles for the LEDs before irradiation (red line) and after the 6 MeV electron irradiation with fluence of 3.5×10^{16} cm^{-2}.

DLTS spectra with quiescent bias of 0.5 V and forward bias pulse of +2 V showed low densities of electron traps with levels E_c–0.5 eV (electron capture cross section of (2–6) $\times 10^{-15}$ cm^2) and E_c–0.7 eV, with electron capture cross section of (3–5)$\times 10^{-15}$ cm^2 [Fig. 3(a)]. In ODLTS spectra measured with 0.5 V bias, the main hole traps had levels near E_v+(0.65–0.68) eV and hole capture cross section of (5–10) $\times 10^{-15}$ cm^2. The centers were the same for the excitation with high-power 455 nm (electrons and holes created mostly in the InGaN QWs) and 365 nm LEDs (excitations in both InGaN QWs and GaN barriers) [Fig. 4(a)].

Electron irradiation to fluencies of 10^{15} and 2×10^{15} cm^{-2} brought no discernible changes in I-V, C-V, and EL characteristics. The deep trap spectra were also not significantly affected. After the fluence of 5×10^{15} cm^{-2} there was increased current in the forward I-Vs, the ideality factor increased from 1.4 to 2.1, and the series resistance in the forward direction increased. The reverse current was not changed [see Figs. 1(a) and 1(b)]. The concentration profile in C-Vs was slightly shifted and broadened (Fig. 2). In DLTS spectra, electron traps at E_c–0.7 eV dominated and an additional peak near Ec-0.2 eV attributed to radiation defects in n-GaN appeared [Fig. 3(a)]. The magnitude of the major hole trap signal at E_v+0.65 eV did

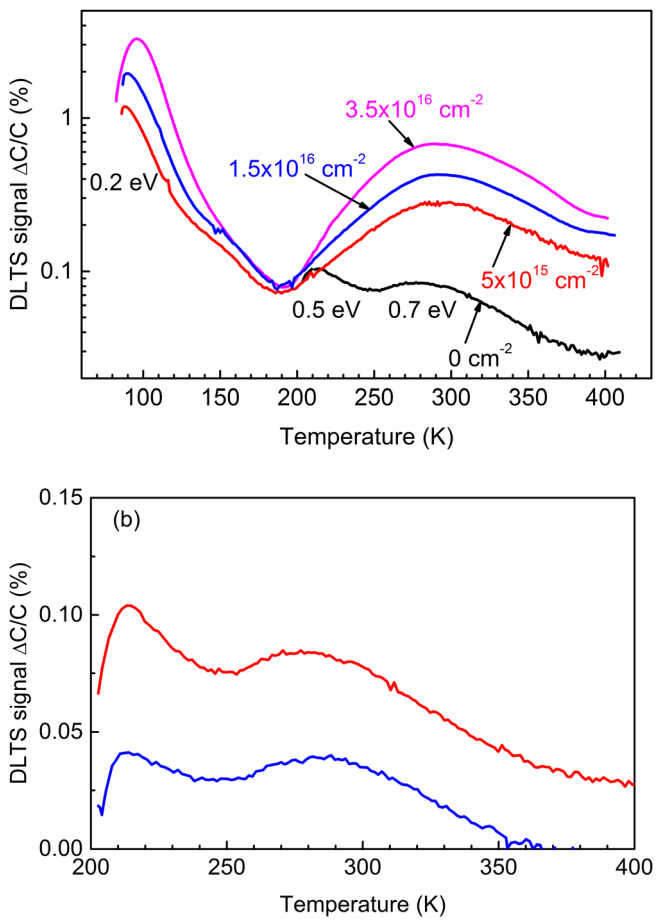

FIG. 3. (a) DLTS spectra measured for blue LEDs before irradiation (black line), after irradiation with 5×10^{15} cm^{-2} 6 MeV electrons (red line), 1.5×10^{16} cm^{-2} (blue line), and 3.5×10^{16} cm^{-2} (magenta line); measurements at 0.5 V, pulse +2 V (3 s), probing frequency 50 kHz; time windows 1.75 s/17.5 s; (b) the effect on DLTS signal before irradiation of constant irradiation with high-power 365 nm LED.

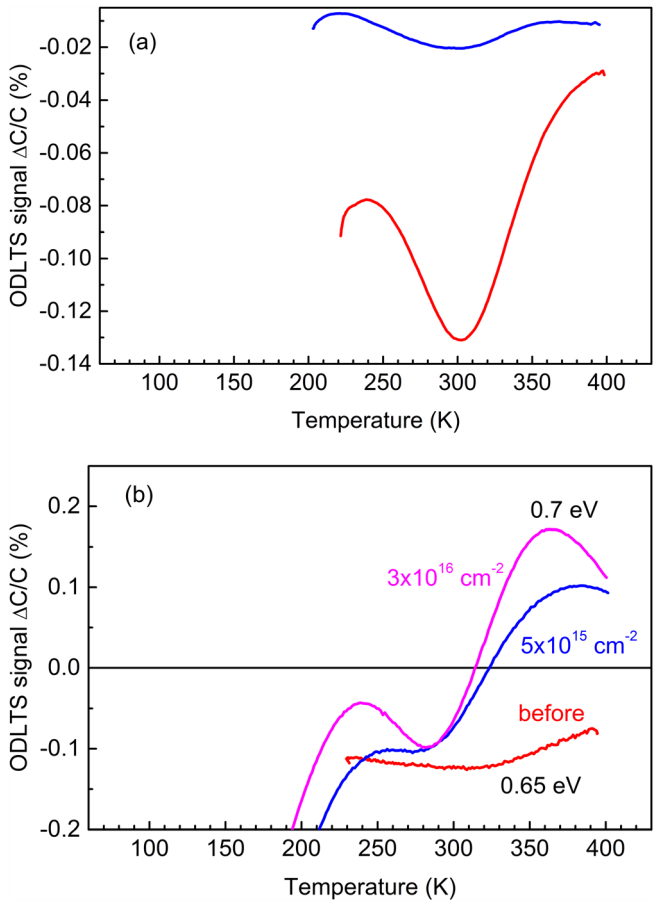

FIG. 4. (a) ODLTS spectra taken before irradiation at 0.5 V, with 455 nm LED excitation (blue line) and 365 nm LED excitation (red line), time windows 100 ms/1000 ms; (b) ODLTS spectra taken with 365 nm LED excitation before irradiation (red line), after irradiation with 5×10^{15} cm^{-2} 6 MeV electron fluence (blue line), and after irradiation with 3×10^{16} cm^{-2} (magenta line).

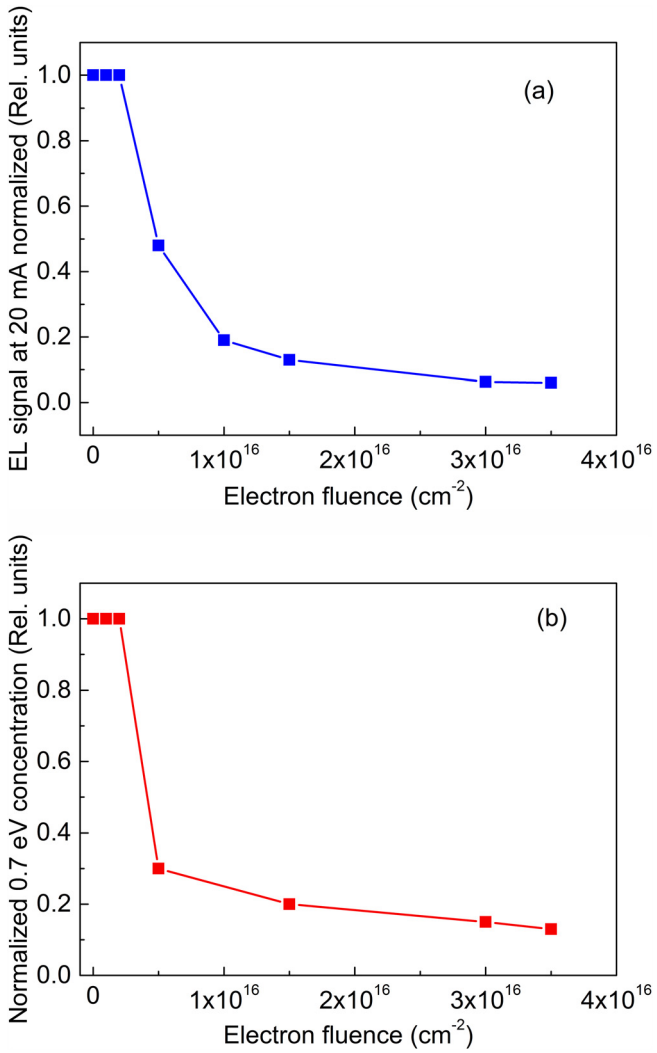

FIG. 5. (a) EL intensity with the LED driving current of 20 mA normalized to the pre-irradiation value shown as a function of fluence; (b) normalized magnitude of the E_c-0.7 eV electron traps as a function of fluence.

not change much (Fig. 4(b); we compared the signal magnitudes for the 365 nm LED excitation because the detected traps were the same for the 455 nm and the 365 nm wavelength excitation, but with the 365 nm excitation it was easier to achieve the signal saturation with the increase of the LED output power). The EL intensity strongly decreased (Fig. 5(a) shows the EL signal at the LED current of 20 mA normalized to the starting value).

Further irradiation did not affect the C-Vs (Fig. 2 shows the profile after the highest electron fluence of 3.5×10^{16} cm^{-2}). The forward and reverse current and series resistance all increased with irradiation fluence [Figs. 1(a) and 1(b)]. The E_c–0.7 eV trap signal increased with electron fluence (Fig. 3(a) shows spectra after fluences of 5×10^{15} cm^{-2}, 1.5×10^{16} cm^{-2}, and 3.5×10^{16} cm^{-2}). The EL signal progressively decreased with increasing electron fluence and approximately followed the trend in the change of relative concentration of the E_c–0.7 eV electron traps [compare the relative changes in the EL signal normalized to the starting value in Fig. 5(a) and the normalized changes in the DLTS peak amplitude normalized to the pre-irradiation value for the E_c–0.7 eV electron traps in Fig. 5(b)]. There was little change in the signal of the major hole traps in ODLTS, although the spectra were distorted by the growing contribution of the signal from the E_c–0.7 eV electron traps [Fig. 4(b)].

IV. DISCUSSION

The most important point is the correlation between the decrease in relative EL power of the LEDs and the relative magnitude of the DLTS signal due to the E_c–0.7 eV electron traps. The EL signal decreases more rapidly than the concentration of the E_c–0.7 eV traps increases, most likely owing to the increase in the series resistance and forward current for low voltages. This current showed only a slight temperature dependence, indicating a strong tunneling or leakage component to the process; such excessive current does not contribute to effective injection and causes additional IQE degradation that is stronger for lower driving current.[24,25] The observed correlation between the density of the E_c–0.7 eV traps and the EL signal after irradiation suggests that these traps are effective recombination centers. This is corroborated by the fact that the E_c–0.7 eV signal can be quenched by constant illumination creating holes during the DLTS measurements. Qualitatively, this can be understood if these are effective SRH recombination centers that are more difficult to recharge with electrons in the presence of holes produced by illumination (similar phenomenon has been reported for the Ec-0.56 eV and

the Ec-1 eV electron traps in n-GaN[10–12]). This center is relatively close to the conduction band edge, and thus, the multiphonon nonradiative hole capture to the center should be handicapped.[6,28] There may be participation of excited states from other charge states of the defect, as in the case of Fe acceptors in GaN.[32,33] It has to be theoretically demonstrated that multiphonon hole capture to the excited states can account for the dramatic increase in hole capture.[20]

Another option is that the E_c–0.7 eV centers capture holes slowly, persistently decreasing the electron injection efficiency into the QWs (thermal emission times from the traps are slow even above room temperatures and would handicap the AC signal; moreover, spatial variations of the traps density can produce potential fluctuations similar to those that are related to local In concentration changes which affect efficiency.[41] In n-GaN and NUV GaN/InGaN LEDs, a similar correlation between the lifetime/EL efficiency and the density of traps far removed from the valence band has been observed.[10–12,24,25,29] The average bulk concentration of the E_c–0.7 eV concentration is $\sim 10^{16}\,cm^{-3}$, more than an order of magnitude higher than prior to irradiation. Participation of the E_c–0.2 eV traps in recombination is excluded because it is difficult to reconcile their effective capture of both electrons and holes in the framework of the multiphonon recombination mechanism. Some other deeper centers could be at play, but the phocapacitance changes in our samples are low, precluding the active contribution by centers not detected in DLTS. The role of dominant hole traps in blue LEDs on EL changes with radiation can likely be discarded because their concentration is too small, even if they were effective recombination centers in InGaN. This is consistent with calculations suggesting that electron capture by such traps can become important for In compositions far into the green-red spectral region.[6]

V. CONCLUSIONS

For high-quality blue GaN/InGaN MQW LEDs, the degradation of EL efficiency upon irradiation with high energy 6 MeV electrons is strongly correlated with an increase in concentration of deep electron traps near E_c–0.7 eV that are effective SRH nonradiative recombination centers.

ACKNOWLEDGMENTS

The work at NUST MISiS was supported in part by the Ministry of Education and Science of the Russian Federation *in the framework of* Increase Competitiveness Program of NUST(MISiS) (K2-2014-055). The work at Korea University was supported by the National Research Foundation of Korea (NRF) funded by Ministry of Science, ICT & Future Planning (2017R1A2B3006141). The work at UF was supported by DTRA Grant No. HDTRA1-17-1-0011.

[1]S. Nakamura and M. R. Krames, Proc. IEEE **101**, 2211 (2013).
[2]C. Shen, T. K. Ng, C. Lee, J. T. Leonard, S. Nakamura, J. S. Speck, S. P. DenBaars, A. Y. Alyamani, M. M. El-Desouki, and B. S. Ooi, Proc. SPIE **10104**, 101041U (2017).
[3]S. H. Oh, B. P. Yonkee, M. Cantore, R. M. Farrell, J. S. Speck, S. Nakamura, and S. P. DenBaars, Appl. Phys. Express **9**, 102102 (2016).
[4]M. Kneissl, "A brief review of III-nitride UV emitter technologies and their applications," in *III-Nitride Ultraviolet Emitters*, edited by M. Kneissl and J. Rass (Springer International Publishing, Switzerland, 2016), Chap. 1.
[5]L. Jun-Lin, Z. Jian-Li, W. Guang-Xu, M. Chun-Lan, X. Long-Quan, D. Jie, Q. Zhi-Jue, W. Xiao-Lan, P. Shuan, Z. Chang-Da, W. Xiao-Ming, F. Wen-Qing, and J. Feng-Yi, Chin. Phys. B **24**(6), 067804 (2015).
[6]C. E. Dreyer, A. Alkauskas, J. L. Lyons, J. S. Speck, and C. G. Van de Walle, Appl. Phys. Lett. **108**, 141101 (2016).
[7]C. Mounir and U. T. Schwarz, Appl. Phys. Lett. **110**, 011106 (2017).
[8]E. Kioupakis, D. Steiauf, P. Rinke, K. T. Delaney, and C. G. Van de Walle, Phys. Rev. B **92**, 035207 (2015).
[9]L. Chernyak, A. Osinsky, G. Nootz, A. Schulte, J. Jasinsky, M. Benamara, Z. Liliental-Weber, D. C. Look, and R. J. Molnar, Appl. Phys. Lett. **77**, 2695 (2000).
[10]I.-H. Lee, A. Y. Polyakov, N. B. Smirnov, E. B. Yakimov, S. A. Tarelkin, A. V. Turutin, I. V. Shemerov, and S. J. Pearton, J. Appl. Phys. **119**, 205109 (2016).
[11]I.-H. Lee, A. Y. Polyakov, N. B. Smirnov, E. B. Yakimov, S. A. Tarelkin, A. V. Turutin, I. V. Shemerov, and S. J. Pearton, Appl. Phys. Express **9**, 061002 (2016).
[12]I.-H. Lee, A. Y. Polyakov, E. B. Yakimov, N. B. Smirnov, I. V. Shchemerov, S. A. Tarelkin, S. I. Didenko, K. I. Tapero, R. A. Zinovyev, and S. J. Pearton, Appl. Phys. Lett. **110**, 112102 (2017).
[13]A. Y. Polyakov, N. B. Smirnov, A. V. Govorkov, H. Amano, S. J. Pearton, I.-H. Lee, Q. Sun, J. Han, and S. Yu. Karpov, Appl. Phys. Lett. **98**, 072104 (2011).
[14]A. R. Arehart, A. Sasikumar, G. D. Via, B. Poling, B. Winningham, E. R. Heller, D. Brown, Y. Pei, F. Recht, U. K. Mishra, and S. A. Ringel, Solid-State Electron. **80**, 19 (2013).
[15]A. Sasikumar, A. R. Arehart, S. Martin-Horcajo, M. F. Romero, Y. Pei, D. Brown, F. Recht, M. A. diForte-Poisson, F. Calle, M. J. Tader, S. Keller, S. P. DenBaars, U. K. Mishra, and S. A. Ringel, Appl. Phys. Lett. **103**, 033509 (2013).
[16]I.-H. Lee, A. Y. Polyakov, N. B. Smirnov, C.-K. Hahn, and S. J. Pearton, J. Vac. Sci. Technol. B **32**, 050602 (2014).
[17]A. Y. Polyakov and I.-H. Lee, "Deep traps in GaN-based structures as affecting the performance of GaN devices (a review)," Mater. Sci. Eng. (R) **94**, 1 (2015).
[18]A. Y. Polyakov, N. B. Smirnov, A. V. Govorkov, and S. J. Pearton, Appl. Phys. Lett. **83**, 3314 (2003).
[19]T. K. Uzdavinys, S. Marcinkevicius, J. H. Leach, K. R. Evans, and D. C. Look, J. Appl. Phys. **119**, 215706 (2016).
[20]I.-H. Lee, A. Y. Polyakov, N. B. Smirnov, R. A. Zinovyev, K.-B. Bae, T.-H. Chung, S.-M. Hwang, J. H. Baek, and S. J. Pearton, Appl. Phys. Lett. **110**, 192107 (2017).
[21]A. Y. Polyakov, I.-H. Lee, N. B. Smirnov, A. V. Govorkov, E. A. Kozhukhova, and S. J. Pearton, J. Appl. Phys. **109**, 123701 (2011).
[22]I.-H. Lee, A. Y. Polyakov, N. B. Smirnov, A. S. Usikov, H. Helava, Y. N. Makarov, and S. J. Pearton, J. Appl. Phys. **115**, 223702 (2014).
[23]M. Meneghini, C. de Santi, N. Trivellin, K. Orita, S. Takigawa, T. Tanaka, D. Ueda, G. Meneghesso, and E. Zanoni, Appl. Phys. Lett. **99**, 093506 (2011).
[24]I.-H. Lee, A. Y. Polyakov, S.-M. Hwang, N. M. Shmidt, E. I. Shabunina, N. A. Tal'nishnih, N. B. Smirnov, I. V. Shchemerov, R. A. Zinovyev, S. A. Tarelkin, and S. J. Pearton, Appl. Phys. Lett. **111**, 062103 (2017).
[25]I.-H. Lee, A. Y. Polyakov, N. B. Smirnov, I. V. Shchemerov, N. M. Shmidt, N. A. Talnishnih, E. I. Shabunina, H.-S. Cho, S.-M. Hwang, R. A. Zinovyev, S. I. Didenko, P. B. Lagov, and S. J. Pearton, "Electron irradiation of near-UV GaN/InGaN light emitting diodes," Phys. Status Solidi A (published online).
[26]M. Meneghini, M. la Grassa, S. Vaccari, B. Galler, R. Zeisel, P. Drechsel, B. Hahn, G. Meneghesso, and E. Zanoni, Appl. Phys. Lett. **104**, 113505 (2014).
[27]A. Y. Polyakov, N. B. Smirnov, E. B. Yakimov, H.-S. Cho, J. H. Baek, A. V. Turutin, I. V. Shemerov, E. S. Kondratyev, and I.-H. Lee, ECS Solid State Sci. Technol. **5**, Q274 (2016).
[28]A. Alkauskas, Q. Yan, and C. G. Van de Walle, Phys. Rev. B **90**, 075202 (2014).
[29]A. Y. Polyakov, N. B. Smirnov, E. B. Yakimov, S. A. Tarelkin, A. V. Turutin, I. V. Shemerov, S. J. Pearton, and I.-H. Lee, J. Alloys Compd. **686**, 1044 (2016).
[30]M. A. Reshchikov and H. Morkoç, J. Appl. Phys. **97**, 061301 (2005).
[31]M. A. Reshchikov, J. Appl. Phys. **115**, 103503 (2014).

[32]D. Wickramaratne, J.-X. Shen, C. E. Dreyer, M. Engel, M. Marsman, G. Kresse, S. Marcinkevičius, A. Alkauskas, and C. G. Van de Walle, Appl. Phys. Lett. **109**, 162107 (2016).
[33]A. Alkauskas, C. E. Dreyer, J. L. Lyons, and C. G. Van de Walle, Phys. Rev. B **93**, 201304(R) (2016).
[34]D.-W. Jeon, L.-W. Jang, H.-S. Cho, K.-S. Kwon, M.-J. Dong, A. Y. Polyakov, J.-W. Ju, T.-H. Chung, J. H. Baek, and I.-H. Lee, Opt. Express **22**(18), 21454–21459 (2014).
[35]M. A. Moram and M. E. Vickers, "X-ray diffraction of III-nitrides," Rep. Prog. Phys. **72**, 036502 (2009).
[36]D. Cherns, S. J. Henley, and F. A. Ponce, Appl. Phys. Lett. **78**, 2691 (2001).
[37]S. J. Rosner, E. C. Carr, M. J. Ludowise, G. Girolami, and H. I. Erikson, Appl. Phys. Lett. **70**, 420 (1997).
[38]J. L. Pautrat, B. Katircioglu, N. Magnea, D. Bensahel, J. C. Pfister, and L. Revoil, Solid-State Electron. **23**, 1159 (1980).
[39]G. M. Martin, A. Mitonneau, D. Pons, A. Mircea, and D. W. Woodard, J. Phys. C: Solid State Phys. **13**, 3855 (1980).
[40]A. Y. Polyakov, N. B. Smirnov, I.-H. Lee, and S. J. Pearton, J. Vac. Sci. Technol. B **33**, 061203 (2015).
[41]F. Nippert, S. Y. Karpov, G. Callsen, B. Galler, T. Kure, C. Nenstiel, M. R. Wagner, M. Straßburg, H.-J. Lugauer, and A. Hoffmann, Appl. Phys. Lett. **109**, 161103 (2016).